Flexible and Printed Electronics

Shellac-paper composite as a green substrate for printed electronics

Flexible and Printed Electronics

PAPER

Shellac-paper composite as a green substrate for printed electronics

Rahaf Nafez Hussein, Kory Schlingman, Calum Noade, R Stephen Carmichael and Tricia Breen Carmichael*

Department of Chemistry and Biochemistry, University of Windsor, Traditional Territory of the Three Fires Confederacy of First Nations, Windsor, Ontario, N9B 3P4, Canada

* Author to whom any correspondence should be addressed.

E-mail: tbcarmic@uwindsor.ca

Keywords: printed electronics, flexible electronics, green electronics, paper electronics, shellac

Supplementary material for this article is available online

OPEN ACCESS

RECEIVED
3 October 2022

REVISED
21 October 2022

ACCEPTED FOR PUBLICATION
2 November 2022

PUBLISHED
14 November 2022

Abstract

Printed electronic (PE) devices that sense and communicate data will become ubiquitous as the Internet of things continues to grow. Devices that are low cost and disposable will revolutionize areas such as smart packaging, but a major challenge in this field is the reliance on plastic substrates such as polyethylene terephthalate. Plastics discarded in landfills degrade to form micro- and nanoplastics that are hazardous to humans, animals, and aquatic systems. Replacing plastics with paper substrates is a greener approach due to the biodegradability, recyclability, low cost, and compatibility with roll-to-roll printing. However, the porous microstructure of paper promotes the wicking of functional inks, which adversely affects printability and electrical performance. Furthermore, truly sustainable PE must support the separation of electronic materials, particularly metallic inks, from the paper substrate at the end of life. This important step is necessary to avoid contamination of recycled paper and/or waste streams and enable the recovery of electronic materials. Here, we describe the use of shellac—a green and sustainable material—as a multifunctional component of green, paper-based PE. Shellac is a cost-effective biopolymer widely used as a protective coating due to its beneficial properties (hardness, UV resistance, and high moisture- and gas-barrier properties); nonetheless, shellac has not been significantly explored in PE. We show that shellac has great potential in green PE by using it to coat paper substrates to create planarized, printable surfaces. At the end of life, shellac acts as a sacrificial layer. Immersing the printed device in methanol dissolves the shellac layer, enabling the separation of PE materials from the paper substrate.

1. Introduction

Printed electronics (PE) facilitates the fabrication of next-generation electronics through conventional printing methods, providing a simple and scalable strategy for fabricating low-cost, thin, lightweight, and flexible devices. Printing methods have successfully been used to fabricate devices such as intelligent labels, smart packaging, printed sensor systems, batteries, solar cells, antennas, and light-emitting devices [1–7]. These printed devices are driving the growth of the Internet of things, a system of ubiquitous, connected devices everywhere in the world. PE is forecast to be a 74-billion-dollar industry by 2030, with a steady annual growth [8]. This massive growth, however, will be environmentally devastating if current substrate materials continue to be used. Plastic substrates used in PE, such as polyethylene terephthalate (PET), polyimide (PI) and polyethylene naphthalate, are produced from non-renewable petrochemicals, which contribute to the climate change crisis. At the end of life, most plastics end up in landfills, with less than a third of plastic waste generated globally being recycled [9]. Plastics decompose in the environment into micro- and nanoplastics, which pollute ecosystems and impose hazards to the health of living things [10, 11]. It is thus essential to replace commonly used plastics with

green alternatives that are robust, scalable, and cost-effective, as well as compatible with printing functional materials for PE. Paper is a compelling choice: it is sustainable, biodegradable, highly recycled, and more cost effective ($\sim$0.1 cent dm^{-2}) compared to commonly used plastics such as PET ($\approx$2 cent dm^{-2}) and PI ($\sim$30 cent dm^{-2}) [12]. Nonetheless, paper substrates have not yet replaced plastics because the porous microstructure of paper causes the imbibition and wicking of functional inks, which compromises printability and resolution [12–18]. Furthermore, an ideal green process for end-of-life recycling should separate and reuse electronic materials and recycle the substrate. Although paper is recycled more than PET, the absorption of functional inks into paper makes it more difficult to separate electronic materials from paper than from PET [19–23]. Here, we report the use of shellac as an environmentally friendly planarization layer and sacrificial layer to overcome these challenges.

Paper is typically made by pressing cellulose fibers from wood or plant pulp into sheets, with a microstructure consisting of a mesh of hydrophilic cellulose fibers with porous voids [24]. Graphics printing of pigmented inks on paper is a well-established technology with a widespread existing infrastructure that includes large-scale roll-to-roll manufacturing with high output speed exceeding 100 km h^{-1} [12]. Despite the ubiquity and sophistication of printing pigmented inks on paper, challenges persist with using paper substrates in PE. PE requires an ultra-smooth and non-absorbing paper substrate to achieve the uniformity and printed film quality necessary for high performance of functional inks [25–27]. These attributes are innate to plastic substrates. In contrast, the poor water resistance of paper, originating from the hydroxyl groups of cellulosic fibers, promotes the absorption and wicking of printed functional inks into the paper [28–30]. The resulting inconsistent and disperse coverage of functional inks leads to poor performance, such as low conductivity for conducting inks. The wicking of functional inks also limits the printing resolution [31–33]. Formulating functional inks to control the wettability, surface tension, and viscosity is one approach to minimize these issues; however, this optimization process must be done individually for each functional ink [34, 35]. A more general approach focuses on the paper substrate itself. Planarizing the paper surface by burying its rough surface profile under a layer of hydrophobic coating material minimizes the absorption of inks and improves the resolution of printed features. Polymer layers such as PET, epoxy, silanes, polyurethane, parylene, latex, and fluorinated acrylate deposited on the paper surface fill in the pores of the paper surface to improve printability [13, 21, 31, 36–45]. The resulting planarized substrates have been used for the fabrication of paper-based thermochromic and electrochromic displays, disposable radio frequency identification tags, batteries, transistors, capacitors, light emitting devices and photovoltaic cells [46–53]. Multilayers of materials have also been explored to planarize the paper surface, increase moisture barrier properties, and increase the surface free energy (SFE) to improve printing resolution [12, 54]. Other research has focused on chemical modification of the paper surface to increase its hydrophobicity and thus minimize wicking and improve the resolution of printed functional inks. For example, modifying paper with alkyl- or perfluoroalkyl silanes improved both the resolution and electrical resistance of printed silver inks compared to printing on unmodified paper [55]. Although effective for printability, some surface coatings and modifications may compromise the safety, recyclability, and biodegradability of the paper substrate. For example, fluorinated materials have safety and environmental concerns due to the leaching of fluorinated materials during recycling. Polymer or wax coatings such as polyethylene, polypropylene, latexes of styrene-butadiene copolymer, or paraffin wax can compromise the compostability and/or recyclability of the paper [56].

Bio-based, biodegradable polymer coatings are a promising replacement for synthetic polymers to prepare paper that is both printable and compostable. Despite the common use of biopolymers such as polysaccharides, proteins, lipids, and starches as coatings for paper-based food packaging to improve moisture resistance and extend food shelf life, the use of these green materials in PE is underdeveloped [57–64]. One example of this approach used cellulose nanocrystals to coat cardboard substrates, reducing the surface roughness from 66 nm to 3.6 nm and impeding the diffusion of functional inks to improve printability [65]. Layering other green materials like lignin, proteins, and starches on paper also provide planarization. For example, blends of clay, calcium carbonate, latex, and mineral pigment have been used to planarize paper substrates for gravure printing of transistors [66], and coatings of chitosan with hydroxypropyl methylcellulose on paper enabled the fabrication of silver nanowire electrodes [67]. However, most of these coatings are water soluble, which limits the applicability of aqueous functional inks. Furthermore, even with 'green' coating materials these approaches have not been designed for end-of-life separation of electronic materials from the substrate for clean recycling. Conventional recycling is not equipped to separate electronic materials from paper. For example, metallic ink particles are too heavy to separate by flotation and too small to remove by screening, leading to contamination of both the recycled paper and waste sludges [68, 69]. The paper substrate may be green, but the electronic materials will still present a problem with recycling or composting.

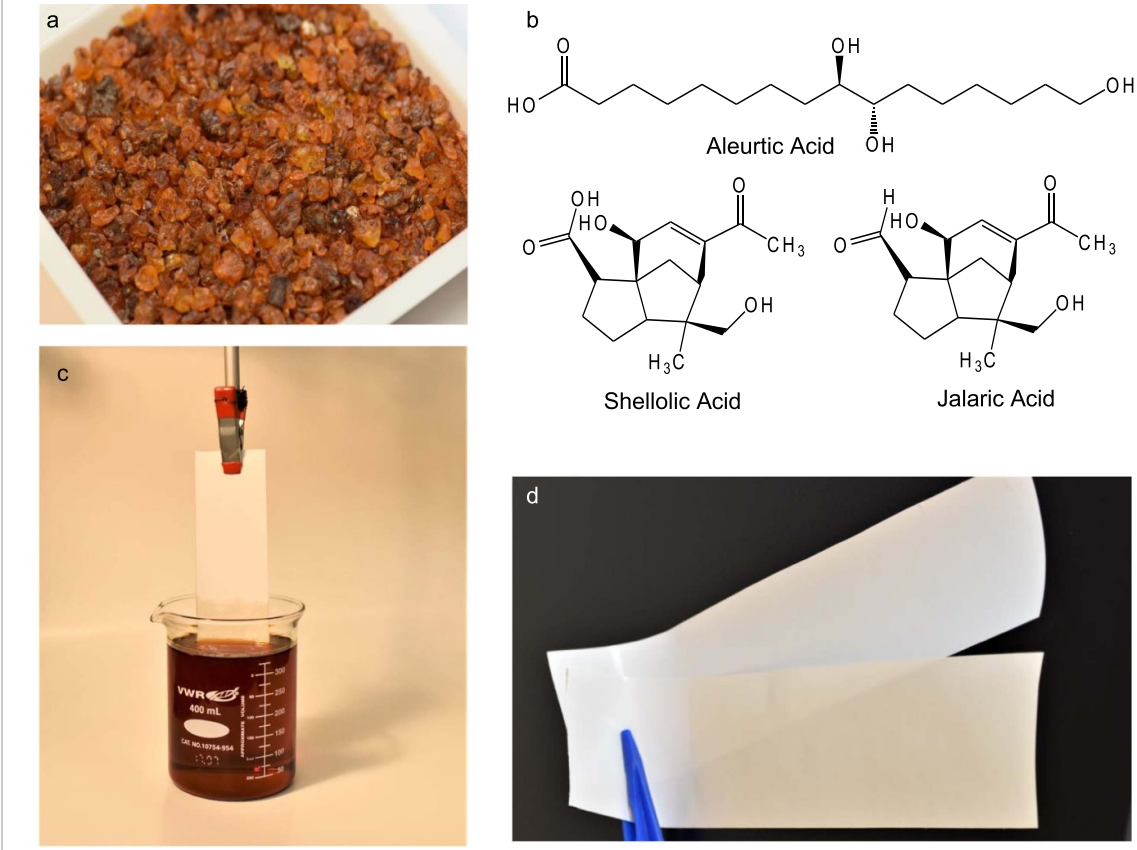

Scheme 1. (a) Photograph of raw seedlac. (b) Chemical structures of the hydroxycarboxylic acids comprising shellac resin. (c) Photograph of dip-coating a paper substrate in shellac solution. (d) Photograph of uncoated paper (top) and SPC-2 (bottom).

Here, we describe the use of shellac as an environmentally friendly, multifunctional coating material to fabricate shellac-paper composite (SPC) substrates for PE. Shellac is a natural bio-polyester thermoplastic resin secreted by a parasitic insect in the family *Kerriidae* (e.g. *Kerria lacca*) on various host trees in India and Thailand [70, 71]. The material obtained directly from the host trees is seedlac (scheme 1(a)), which is a mixture of mixture of shellac resin (70%–80%), wax (6%–7%), and colorant molecules (4%–8%). Seedlac is soluble in green solvents like alcohols and aqueous basic solutions, enabling the separation of the shellac resin from the other components. Shellac resin is a complex mixture of long chain inter/intra-esters of hydroxycarboxylic acids, primarily aleuritic acid, shellolic acid, and jalaric acid (scheme 1(b)) [72]. Shellac resin is a cost-effective bio-adhesive commonly used as a coating material to provide smooth and glossy surfaces with good hardness, UV resistance, and high moisture- and gas-barrier properties. Shellac is widely used in abrasives, sealing wax, hair sprays, edible glazes, and pharmaceutical coatings [73, 74]. Despite its useful properties, shellac has not been significantly explored in PE. Thin films of shellac have previously been used as a dielectric layer and substrate for printed organic field-effect transistors and as a matrix for electrically conductive inks for the fabrication of disposable graphite-based supercapacitors [75, 76]. In this paper, we use shellac to advance PE by fabricating a new SPC that provides a smooth, uniform surface while imparting high moisture resistance, physical strength, and a SFE well-suited to printability. Subsequent dissolution of the shellac layer in methanol releases the printed layers from the paper substrate for an effective and simple end-of-life process.

2. Results and discussion

We fabricated SPCs by first preparing a shellac solution by dissolving 10 g of Kusmi seedlac in 50 ml anhydrous ethanol and agitating the mixture for 90 min at 150 rpm on an orbital shaker. Leaving the mixture for 24 h allows the debris and insoluble wax particles from the seedlac to settle. Decanting the lacquer followed by filtration produces a clear solution that passes through a 0.20 μm filter (figure S1). This process yields an ethanolic shellac lacquer with a concentration of 200 mg ml^{-1} and a viscosity of ~2.5 cP. We fabricated the SPCs by dip-coating a paper substrate into the shellac lacquer (scheme 1(c), supplementary video V1). The paper substrate is a calendared uncoated paper with a grammage of ~67 g m^{-2} and a thickness of ~30 μm. After dip-coating, we allowed the solvent to evaporate at room

Table 1. Thicknesses, basis weight, bulk densities, and dry coat weights uncoated paper, SPC-1, and SPC-2 ($n = 15$).

Substrate	Coating thickness (μm)	Basis weight (g m^{-2})	Dry coat weight (g m^{-2})
Uncoated paper	0	67.2 ± 0.3	0
SPC-1	<10	70.8 ± 0.3	3.6 ± 0.1
SPC-2	10.2 ± 1.2	74.6 ± 0.4	7.2 ± 0.2

temperature. We studied composites made with a single
dip-coated layer of shellac (SPC-1), and composites made with two dip-coated layers of shellac (SPC-2). Both SPC-1 and SPC-2 composites appear uniform and glossy, with a smooth texture (scheme 1(d)). After dip-coating, the bulk density of SPC-1 and SPC-2 increased compared to the uncoated paper (table 1). The dry coat weight of SPC-2 is double that of SPC-1, indicating that shellac can be layered onto paper through consecutive dip/dry cycles. Using thicker coatings of shellac by increasing the number of dip coats or concentration of the lacquer is not beneficial. Thicker layers not only add weight—an important consideration in smart packaging—but also impart the inherent brittleness of shellac to the composites, which visibly crack when handled (figure S2).

SEM images of the uncoated paper and SPCs show that the shellac coating covers the texture of the paper substrate. Images of the paper substrate alone reveal the grainy texture in which the grains have distinct edges (figure 1(a)). The SEM image (figure 1(b)) of SPC-1 shows that a single coating of shellac does not appreciably change the appearance of the grains. The second coating of shellac of SPC-2, however, softens the edges of the grains and provides a more homogeneous-looking surface (figure 1(c)). We determined the shellac coating thickness of SPC-2 using cross-sectional SEM (figure 1(d)). The image shows the shellac coating, which appears as the lighter color fully coating both sides of the paper substrate. The contrast between the shellac layers sandwiched around the paper substrate indicates that the shellac mainly coats the paper surface. The thickness of the shellac coating is $\sim$10 μm, while the coating thickness of SPC-1 was too thin to assess using cross-sectional SEM. Both SPC-1 and SPC-2 are robust to scratching and exhibit strong adhesion between the shellac layer and paper, likely due to adhesive forces and mechanical interlock between the shellac layer and rough paper surface. The tape peel test tears the paper substrate without delamination of the shellac coating.

We used atomic force microscopy (AFM) to quantify the planarization provided by the shellac coatings in SPC-1 and SPC-2 (figure 2). AFM images of the uncoated paper substrate show a rough

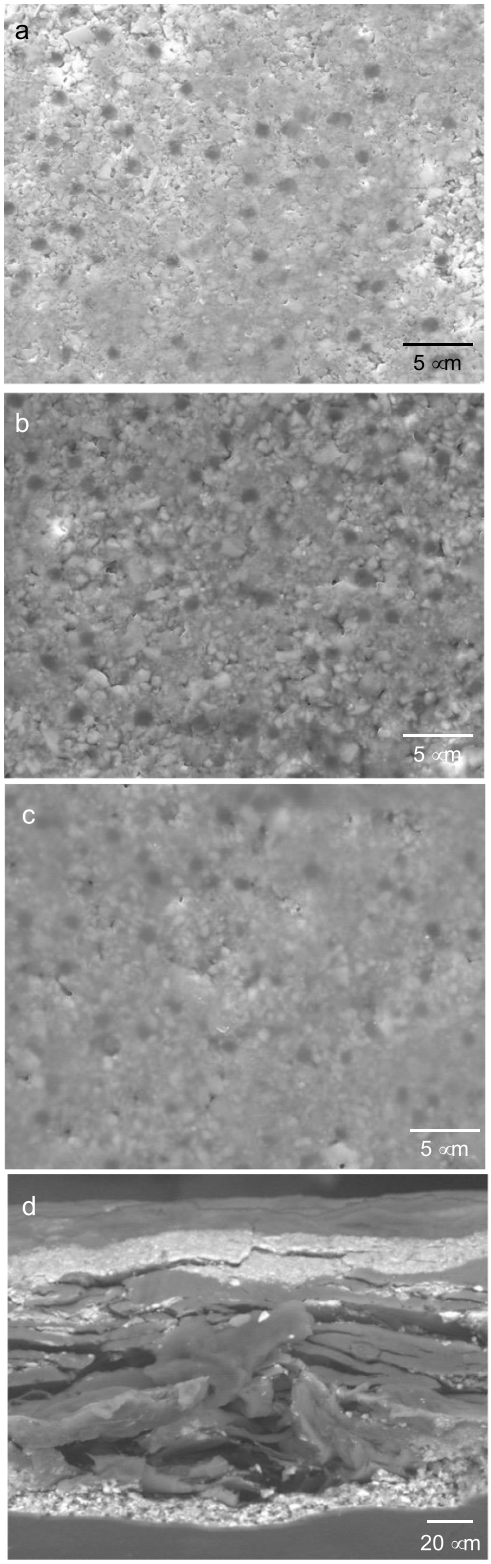

Figure 1. SEM micrographs of (a) uncoated paper substrate, (b) SPC-1, (c) SPC-2. (d) Cross-sectional SEM image of SPC-2.

substrate with deep voids consistent with the grainy texture in the SEM images. Uncoated paper has a root-mean-square (RMS) roughness value of 420 ± 30 nm and a peak-to-valley distance of $\sim$1.6 μm. AFM images of SPC-1 and SPC-2 show

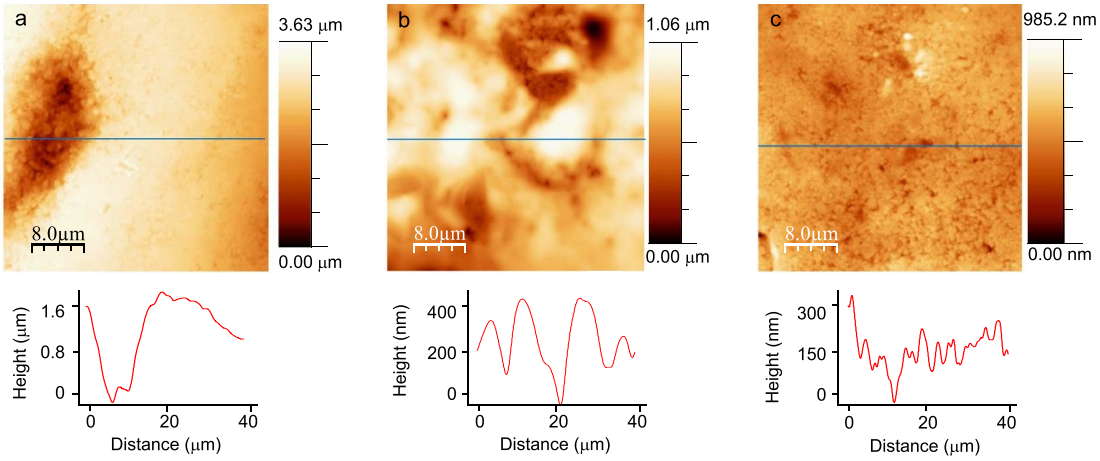

Figure 2. AFM height images and profiles of (a) uncoated paper substrate, (b) SPC-1, (c) SPC-2. The blue lines on the height images show the profile location.

that the shellac coating fills in the void spaces on the surface of the paper substrate to reduce the roughness. One coating of shellac in SPC-1 reduces the peak-to-valley distance to ∼400 nm, with an RMS roughness value of 170 ± 30 nm. Two coats of shellac in SPC-2 further reduce the RMS roughness to 78 ± 7 nm with maximum peak-to-valley distances of ∼250 nm.

Adding shellac layers to paper in SPC-1 and SPC-2 increases both the stiffness and strength of the substrate while maintaining mechanical flexibility. In the paper making process, the cellulose fibers orient in the direction of the flow of the pulp leading to an anisotropic structure with long fibers aligned in the machine direction (MD) and shorter fibers aligned perpendicular to the MD (the cross direction (CD)) [77, 78]. We quantified the mechanical properties of uncoated paper, SPC-1, and SPC-2 by tensile test in both the MD and CD (figure S3). The Young's moduli increase in both directions as shellac layers are added to the paper substrate (figure 3(a)). For all three substrates, the Young's moduli are higher in the MD compared to the CD. This anisotropy is inherent to the paper substrate; however, the disparity between the Young's moduli in the MD and CD diminishes with the addition of shellac coatings. The well-adhered shellac layer acts as a reinforcement to the paper substrate to minimize the anisotropy in the mechanical properties. This effect is also evident in the tensile index (TI), the maximum tensile force per unit width and unit grammage. TI is a common way to express the strength of a paper substrate during tensile loading. Even with the increased grammage, shellac coatings in SPC-1 and SPC-2 increase the TI in both the MD and CD (figure 3(b)). SPC-2 exhibits a TI ∼2 times greater than that of uncoated paper. The disparity in TI in the MD and CD decreases from a 35% difference for uncoated paper to only 4% for SPC-2.

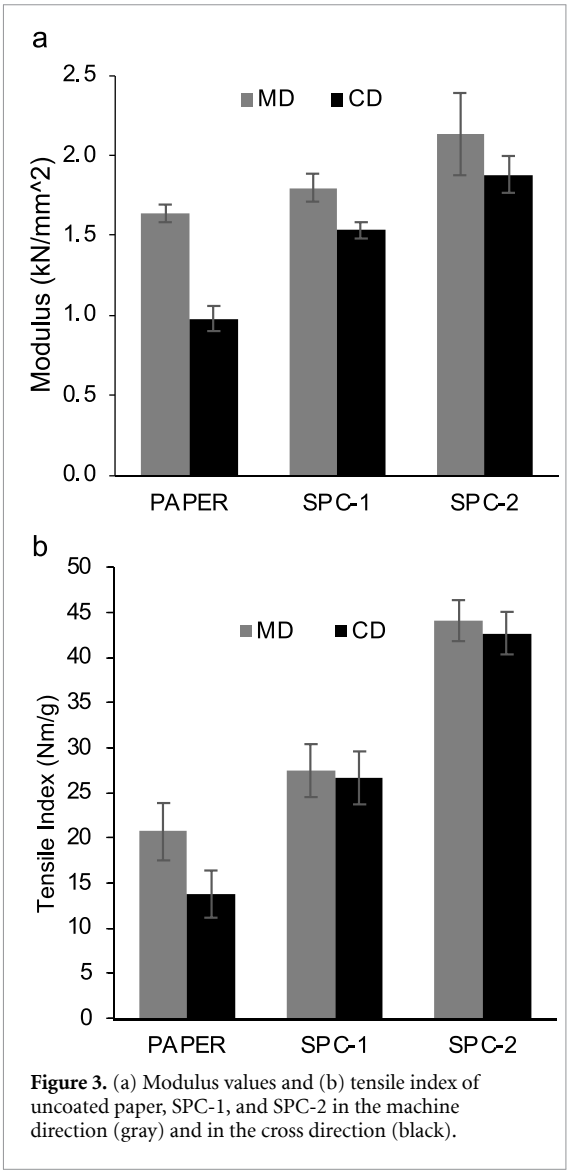

Figure 3. (a) Modulus values and (b) tensile index of uncoated paper, SPC-1, and SPC-2 in the machine direction (gray) and in the cross direction (black).

Mechanical flexibility is a requirement for paper substrates used in PE, as these substrates will ultimately need to tolerate repeated bending during

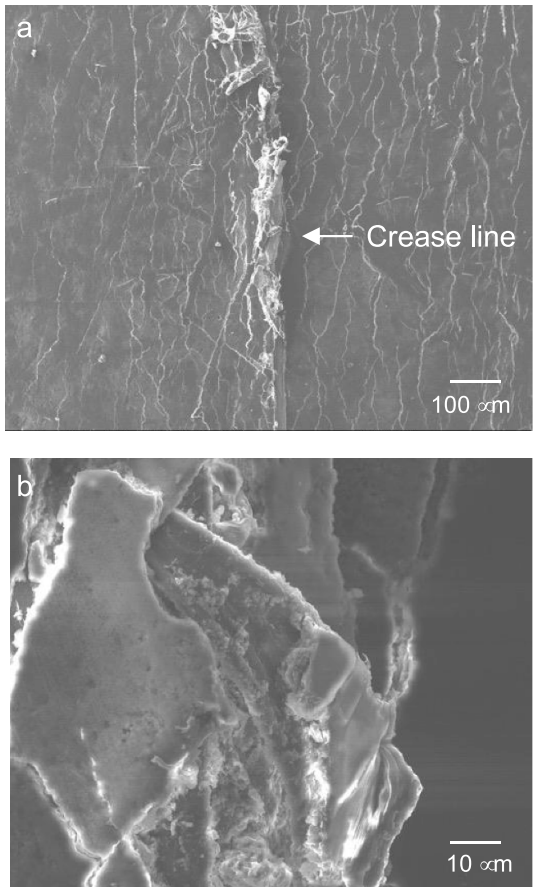

Figure 4. SEM images of SPC-2 after creasing at (a) low and (b) high magnification.

feeding through roll-to-roll printing equipment. Although shellac is an inherently brittle material, the combination of shellac with paper to form the composite provides mechanical flexibility. We assessed the mechanical flexibility of SPC-2 by repeated bending to radii of curvature of 8 mm, 6 mm, 3 mm, and 1.5 mm (supplementary video V2), corresponding to bending strains (ε) of 0.18, 0.25, 0.5, 1 respectively (equation (1), where ε is the bending strain, d is the thickness of the substrate, and r is the radius of the curvature) [79]

$$\varepsilon = d/2r. \quad (1)$$

We assessed the bending of the composite in both the MD and CD and examined the effect of mechanical strain on the shellac coating using SEM. After 1000 bending cycles at each radius of curvature, the composite did not exhibit cracking. Visible damage only resulted from folding SPC-2 to create a crease, which caused micro-tearing of the underlying paper surface, protrusion of cellulose fibers through the shellac coating, and the propagation of microcracks in the shellac coating parallel to the folding line (figures 4(a) and (b)).

The shellac coatings of SPC-1 and SPC-2 are not only smooth and strengthen the paper substrate, but also reduce ink absorption into the paper. Limiting the absorption of functional inks into paper is essential for printability in PE to achieve the uniformity and printed film quality necessary for high performance. We studied the interaction between a drop of water and the surfaces of uncoated paper, SPC-1, and SPC-2 by measuring contact angles over 60 s at the same temperature and relative humidity (figure 5(a)). The contact angle decreases dramatically for water on uncoated paper, reaching a value of 0° within 60 s. The rapid decrease in contact angle can be attributed to the absorption of water into the porous, hydrophilic paper structure. In contrast, the shellac layers in SPC-1 and SPC-2 resist the absorption of water and show only a small decrease in contact angle beginning at ∼50 s, consistent with the superior moisture barrier properties of the shellac-coated surfaces compared to uncoated paper. The time it takes for the contact angle to reach 0° is 8 min and 15 min for SPC-1 and SPC-2, respectively. On these substrates, the decrease in contact angle is due to a combination of absorption and evaporation of the water drop. Two coats of shellac in SPC-2 provide better barrier properties compared to those of SPC-1, consistent with the more uniform coating of shellac in SPC-2 observed in SEM images. The time it takes for the contact angle of water on SPC-2 to reach 0° is comparable to the time it takes for evaporation of the same volume of water on a glass surface (∼20 min).

We further characterized the absorption of inks into uncoated paper, SPC-1, and SPC-2 using a trace color test, in which an aliquot of a dye solution is placed on the front side of the substrate and left to dry. The diameter of the dried ink drop on the front side of the substrate and the area of the ink spot on the back side are indicators of the wicking and absorption of the ink solution. We investigated the absorption of different solvents commonly used in PE using Sudan Red III, a water-insoluble dye, dissolved in dichloromethane, tetrahydrofuran (THF), toluene, and chloroform, and Evans Blue, a water-soluble dye, dissolved in water, acetone, and methanol. Figure 5(b) shows optical images of the front and back sides of uncoated paper, SPC-1, and SPC-2 subjected to the trace color test using Sudan Red III dye dissolved in THF. On the front side, the pigmented ink spreads further on the uncoated paper than on SPC-1 and SPC-2 (figure 5(c)). The back side of the substrates shows a dramatic difference in ink penetration through the substrates. We analyzed the images of the back side of the substrate to determine the % area of ink. This value was lowest on SPC-2 for all solvents tested (figure 5(d)). Methanol penetrated through SPC-2 the most, consistent with the solubility of shellac in methanol.

Printing of functional materials onto substrates requires detailed knowledge of the ink-substrate interactions, wettability, and adhesion between the ink and substrate. The SFE of a substrate is an

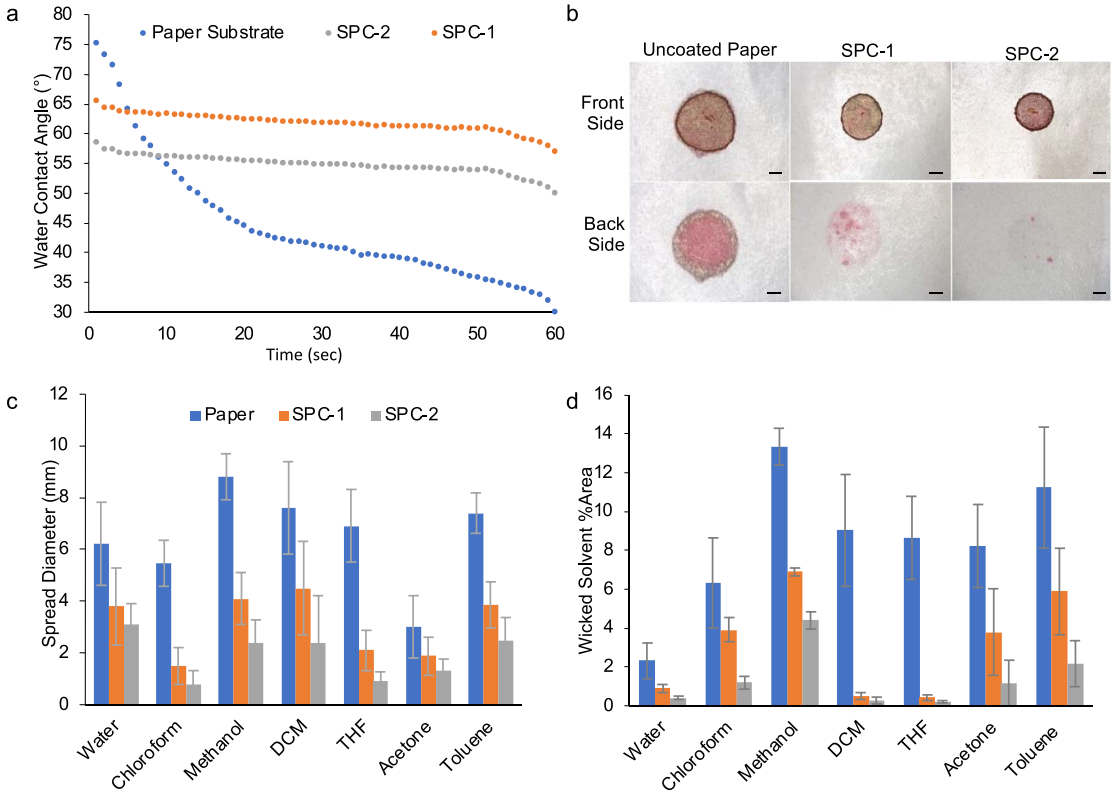

Figure 5. (a) Water contact angles measured over 60 s on uncoated paper (blue), SPC-1 (orange), and SPC-2 (gray). (b) Optical microscope images of front side (top row) and back side (bottom row) of uncoated paper, SPC-1, and SPC-2 after the trace color test with Sudan III dye in THF (scale bar = 1.5 mm). (c) Spreading diameter of the pigment in different solvents on uncoated paper (blue), SPC-1 (orange), and SPC-2 (gray). (d) % Area of trace color that has penetrated through uncoated paper (blue), SPC-1 (orange), and SPC-2 (gray).

important factor controlling the wetting of functional inks on the surface [80]. Wetting requires a close match between the SFE of the printed substrate and the surface tension of the functional ink. Matching these values optimizes the quality of the printed pattern, the printing resolution, and the adhesion of the ink to the substrate. The surface tension of most solvents used in formulating functional inks used in PE ranges between 22 and 37 mN m^{-1}. We determined the applicability of SPC-1 and SPC-2 as substrates in PE using contact angle measurements to calculate SFE values according to the Owens, Wendt, Rabel and Kaelble model [81, 82]. This model is a commonly used SFE theory, in which the interfacial interactions are divided into two parts: polar (γ^p) and dispersive (γ^d). Calculation of the SFE requires the measurement of the contact angle of one polar and one dispersive liquid. We measured contact angles of water as the polar component and diiodomethane as the dispersive component on SPC-1 and SPC-2 (table 2). The SFE values for SPC-1 and SPC-2 of 45.5 ± 0.5 mN m^{-1} and 39.0 ± 0.2 mN m^{-1} are both suitable for PE, with the SFE value for SPC-2 closely matching typical surface tension values for functional inks.

We demonstrated the printability of SPC-1 and SPC-2 by screen printing a water-based silver paint and comparing the properties of the printed films to films printed on uncoated paper and PET. We applied a water-based NO-VOC Silver Paint with a particle size of <20 μm and a 40% loading through a vinyl stencil applied to the surface of the substrate. We patterned silver lines 20 mm in length and 0.2 mm, 0.5 mm, 0.75 mm, 1.5 mm, and 2.0 mm in width (figure 6(a)). We analyzed the printed lines on each substrate using optical microscopy to compare the fidelity of the printed pattern to the vinyl mask (figure 6(b)). The line widths of patterned silver ink on SPC-1, SPC-2, and PET were all close to the nominal line widths, showing that the barrier properties of the shellac coating create a printable surface similar to PET. In contrast, the absorptive, porous nature of uncoated paper results in wicking of the ink, which leads to a loss of fidelity, particularly for narrow lines (0.2, 0.5, and 0.75 mm). Figures 6(c)–(f) shows the differences in quality of 0.2 mm wide printed lines on the four substrates. The shellac coatings on SPC-1 and SPC-2 prevent wicking, and the printed lines are indistinguishable from those on PET. We quantified the blurring of the line edges by determining line edge roughness (LER) values of the silver lines on each substrate. LER values for printed lines on SPC-1, SPC-2, and PET were <0.05 μm, while the LER values of printed lines on uncoated paper

Table 2. Contact angle values and SFEs of SPC-1 and SPC-2 ($n = 10$).

	Contact angle (°)		Surface free energy (mN m^{-1})		
	Water	Diiodomethane	γ^{p}	γ^{d}	γ^{total}
SPC-1	63.5 ± 0.4	53.4 ± 0.6	13.0 ± 0.1	32.6 ± 0.4	45.5 ± 0.5
SPC-2	57.8 ± 0.4	90.1 ± 0.6	29.3 ± 0.1	9.8 ± 0.1	39.0 ± 0.2

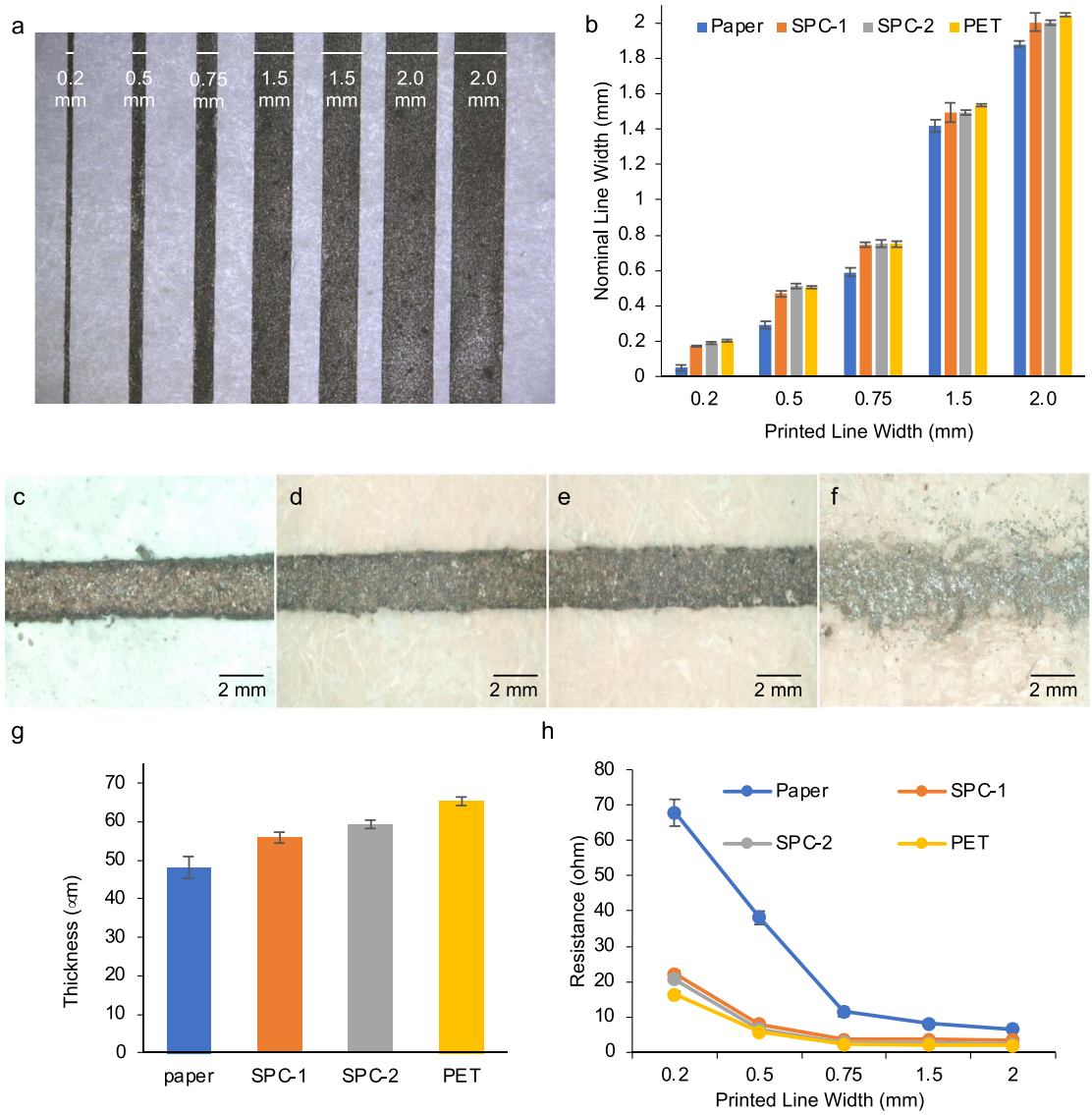

Figure 6. (a) Optical microscope images of printed silver inks on SPC-2. (b) Fidelity of the printed lines on uncoated paper (blue), SPC-1 (orange), SPC-2 (gray), and PET (yellow). Optical microscope images of 0.20 mm wide printed silver lines on (c) PET, (d) SPC-2, (e) SPC-1, (f) uncoated paper. (g) Thickness of printed silver lines on uncoated paper (blue), SPC-1 (orange), SPC-2 (gray), and PET (yellow). (h) Resistance values of silver printed lines of different widths on uncoated paper (blue), SPC-1 (orange), SPC-2 (gray), and PET (yellow).

were notably higher (∼0.2 μm) (figure S4). Optical profilometry shows that printed silver ink on PET is slightly thicker (∼26%) than printed lines on SPC-1 and SPC-2, which are all thicker than printed lines on uncoated paper (figure 6(g)). This trend is consistent with the absorption of the silver ink into uncoated paper and indicates a minor amount of absorption may occur on SPC-1 and SPC-2. This trend is also reflected in the electrical performance of the printed silver lines on each substrate (figure 6(h)). In general, the resistance of the silver lines on each substrate increased as the linewidth decreased. Since resistance is inversely proportional to the cross-sectional area of the conductor, decreasing the linewidth also decreases the cross-sectional area and increases the resistance. At the same linewidth, however, the resistance values of silver lines printed on uncoated paper were notably higher than that of silver lines printed on

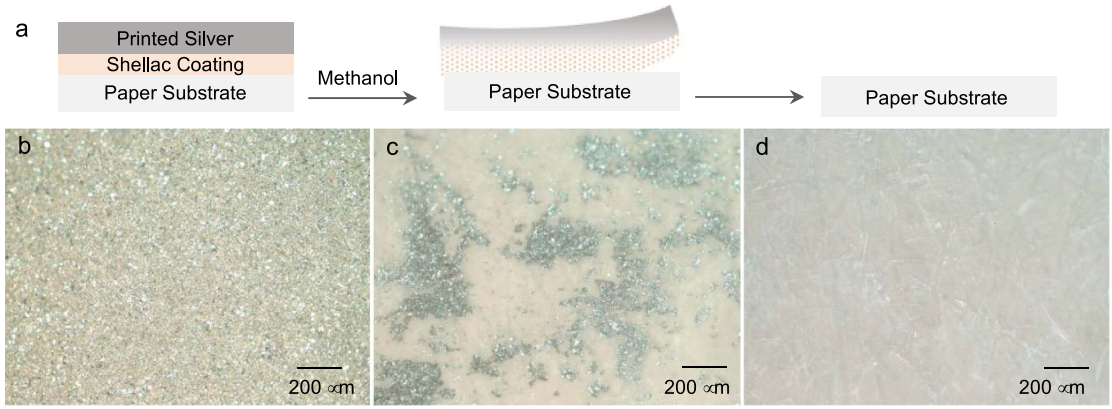

Figure 7. (a) Schematic of the process for removing printed silver ink on SPC-2. Optical images of (b) printed silver SPC-2, (c) after sonication for 2 min in methanol, (d) after sonication for 5 min in methanol.

SPC-1, SPC-2, and PET, consistent with the wicking of the silver ink into the paper. More importantly, the resistance values of silver lines on SPC-1 and SPC-2 were indistinguishable from those on PET, with the PET substrate giving a slight advantage only at the smallest (0.2 mm) linewidths.

For truly green PE, the recyclability of printed devices is essential at the end of life. Printed silver ink is a material of choice due to its high conductivity, which is necessary for devices like printed antennas. However, silver inks entering the recycling process may lead to contamination of recycled paper and/or waste streams. In addition, silver is an expensive metal, making reclamation an important part of sustainable PE. Separating printed silver ink from uncoated paper highlights the challenge: soaking and sonicating silver inks printed on uncoated paper in methanol and filtering the solid material yielded only ∼10% of the mass of printed silver. In contrast, the shellac coating of SPC-2 acts as a sacrificial lift-off layer to efficiently release printed silver inks (figure 7(a)). The shellac coating dissolves in methanol with soaking and sonication, fully lifting the silver ink from the substrate after 5 min. This process recovered ∼95% of the mass of silver from the SPC-2 substrate. Optical micrographs show the lift-off of printed silver ink on SPC-2 (figures 7(b)–(d)).

3. Conclusions

The development of environmentally conscious materials and methods for PE is critically important to protect the planet from the detrimental effects of discarded PE devices.

The shellac coatings on paper demonstrated in this work use a sustainable, green natural product to produce printable paper substrates that are not only eco-friendly, but also facilitate the separation of electronic materials at the end of life. The dip-coating method to apply shellac coatings to paper is scalable; furthermore, other scalable application methods like spray-coating and roll printing are promising for the large-scale, economical preparation of SPCs. The use of SPCs in PE manufacturing will mature with demonstrations of an expanded range of functional printing inks and printing methods.

4. Methods

Kusmi seedlac was obtained from Wood Finish Supply (Napa). Biaxially oriented PET (Goodfellow, 0.05 mm thickness). All other chemicals were obtained from Sigma-Aldrich and were used as received.

4.1. Formulation of shellac solution

A 200 mg ml^{-1} shellac solution was prepared by dissolving 10 g of Kusmi seedlac in 50 ml anhydrous ethanol and agitating the mixture for 90 min at 150 rpm using an orbital shaker (IKA KS 130). The mixture was then left for 24 h to allow the waxes and debris to settle. The lacquer was then decanted and filtered through a series of filter papers with successively smaller pore sizes to remove wax and debris from the solution. A final filtration through a 220 nm PTFE syringe filter yields an ethanolic shellac lacquer with a concentration of 200 mg ml^{-1} and a viscosity of ∼2.5 cP.

4.2. Fabrication of shellac/paper composites

Paper substrates were cleaned in anhydrous ethanol for 5 min with sonication and then left to dry. A homemade robotic arm was used for dip coating (supplementary video V1). The cleaned paper substrates were dipped in a reservoir of 200 mg ml^{-1} of shellac at a speed of 0.60 cm s^{-1} and a dwell time of 10 s in the reservoir. The samples were then lifted out of shellac solution at 0.60 cm s^{-1} and left to dry in

air for 15 min. This process was then repeated for a double-layer shellac coating.

4.3. Printing of silver ink

Printing of silver ink was sonicated in water for 5 min and left to dry. Adhesive vinyl stencils were fabricated using a vinyl cutter, and then laminated on the surface of uncoated paper, SPC-1, and SPC-2 substrates. About 0.70 g of SPI Supplies NO-VOC Silver Paint was deposited on the stencil, and the excess was removed with a silicone rubber squeegee. The printed substrate was then left to air dry for 10 min, then the vinyl mask was peeled off and the substrate was sintered on a hotplate for 10 min at 60 °C.

4.4. Removal of silver ink

Printed substrates were placed in methanol and sonicated in Branson sonicator (Model 3510) for 5 min. The silver precipitate was then collected by vacuum filtration.

5. Characterization

SEM images are collected using a Quanta 200 FEG Environmental SEM. SPC-1 and SPC-2 samples were cut with a microtome for cross-sectional imaging. AFM images were collected using a Digital Instruments Multimode AFM in tapping mode. A FESP cantilever with a tip of 8 nm radius and force constant of 2.8 N m^{-1} was used. AFM images were collected over a 40 μm × 40 μm scan area using a scan rate of 0.5 Hz and a scanning resolution of 512 samples/line. RMS roughness values from three different areas of a sample were averaged. Roughness measurements were determined using WSxM 5.0 Develop 10.2 software [83]. The reported roughness is an average of at least three values. Contact angles were measured using the sessile drop method on a Rame-Hart contact angle goniometer at 23 °C and 17% relative humidity. Stress/strain properties were tested using an MTS Criterion Model 43 tensile tester and the procedure ASTM D828; reported values are the median of six measurements. Repetitive bending tests were done using a home-made auto-stretching stage (supporting video V2). For trace color analysis, quantification of the amount of trace color on the back side of the substrates determined by ImageJ analysis of optical images. Resistance measurements of printed silver inks were taken using a Keithley 2601A SourceMeter. LER of printed silver ink was obtained by analyzing optical images using the Analyze Stripes macro (Bickford, 2013) for ImageJ. The reported LER is an average of RMS LER values from six images.

Data availability statement

The data that support the findings of this study are available upon reasonable request from the authors.

Acknowledgments

This research was supported by the National Sciences and Engineering Research Council of Canada (NSERC) through the Green Electronics Network (GreEN) (NETGP 508526-17). The authors thank Calvin Love for building the dip coating apparatus.

ORCID iD

Tricia Breen Carmichael https://orcid.org/0000-0002-0847-437X

References

[1] Shrestha K, Kim Y, Jung Y, Kim S, Truong H and Cho G 2021 Wireless pH-logger label for intelligent food packaging *Flex. Print. Electron.* **6** 044001
[2] Sowade E, Polomoshnov M, Willert A and Baumann R R 2019 Toward 3D-printed electronics: inkjet-printed vertical metal wire interconnects and screen-printed batteries *Adv. Eng. Mater.* **21** 1900568
[3] Kim Y Y, Yang T Y, Suhonen R, Välimäki M, Maaninen T, Kemppainen A, Jeon N J and Seo J 2019 Gravure-printed flexible perovskite solar cells: toward roll-to-roll manufacturing *Adv. Sci.* **6** 1802094
[4] Salmerón J F, Molina-Lopez F, Briand D, Ruan J J, Rivadeneyra A, Carvajal M A, Capitán-Vallvey L F, de Rooij N F and Palma A J 2014 Properties and printability of inkjet and screen-printed silver patterns for RFID antennas *J. Electron. Mater.* **43** 604–17
[5] An K 2019 High speed nozzle jet printing for bendable organic light emitting diodes *Flex. Print. Electron.* **4** 015009
[6] Zhang L, Wang H, Zhao Y, Guo Y, Hu W, Yu G and Liu Y 2013 Substrate-free ultra-flexible organic field-effect transistors and five-stage ring oscillators *Adv. Mater.* **25** 5455–60
[7] Wang X, Zheng S, Zhou F, Qin J, Shi X, Wang S, Sun C, Bao X and Wu Z-S 2020 Scalable fabrication of printed Zn//MnO_2 planar micro-batteries with high volumetric energy density and exceptional safety *Nat. Sci. Rev.* **7** 64–72
[8] Das R and He X 2020 Flexible, printed and organic electronics 2020–2030: forecasts, technologies, markets *IDTechEx* (available at: www.idtechex.com/en/research-report/flexible-printed-and-organic-electronics-2020-2030-forecasts-technologies-markets/687)
[9] Geyer R, Jambeck J R and Law K L 2017 Production, use, and fate of all plastics ever made *Sci. Adv.* **3** e1700782
[10] Leslie H A, van Velzen M J M, Brandsma S H, Vethaak A D, Garcia-Vallejo J J and Lamoree M H 2022 Discovery and quantification of plastic particle pollution in human blood *Environ. Int.* **163** 107199
[11] Mattsson K, Jocic S, Doverbratt I and Hansson L A 2018 Nanoplastics in the aquatic environment *Microplastic Contamination in Aquatic Environments* ed E Y Zeng (Amsterdam: Elsevier) ch 13, pp 379–99
[12] Tobjörk D and Österbacka R 2011 Paper electronics *Adv. Mater.* **23** 1935–61
[13] Trnovec B, Stanel M, Hahn U, Hübler A C, Kempa H and Sangl R 2009 Coated paper for printed electronics *Prof. Papermak.* **1** 48–51
[14] Ihalainen P, Määttänen A, Järnström J, Tobjörk D, Österbacka R and Peltonen J 2012 Influence of surface properties of coated papers on printed electronics *Ind. Eng. Chem. Res.* **51** 6025–36
[15] Nechita P 2020 The influence of drying conditions of clay-based polymer coatings on coated paper properties *Coatings* **11** 12
[16] Aydemir C, Kašikovic N, Horvath C and Durdevic S 2021 Effect of paper surface properties on ink color change, print

gloss and light fastness resistance *Cellul. Chem. Technol.* **55** 133–9
[17] Xu Y *et al* 2020 Pencil–paper on-skin electronics *Process. Nat. Acad. Sci.* **117** 18292–301
[18] Dong Y, Wang B, Ji H, Zhu W, Long Z and Dong C 2020 Effect of papermaking conditions on the ink absorption and overprint accuracy of paper *BioResources* **15** 1397–406
[19] Wäger P A, Eugster M, Hilty L M and Som C 2005 Smart labels in municipal solid waste—a case for the precautionary principle? *Environ. Impact. Assess. Rev.* **25** 567–86
[20] Aliaga C, Zhang H, Dobon A, Hortal M and Beneventi D 2015 The influence of printed electronics on the recyclability of paper: a case study for smart envelopes in courier and postal services *Waste Manage.* **38** 41–48
[21] Li J, Shrivastava P, Gao Z and Zhang H C 2004 Printed circuit board recycling: a state-of-the-art survey *IEEE Trans. Electron Packag. Manuf.* **27** 33–42
[22] Glogic E, Futsch R, Thenot V, Iglesias A, Joyard-Pitiot B, Depres G, Rougier A and Sonnemann G 2021 Development of eco-efficient smart electronics for anticounterfeiting and shock detection based on printable inks *ACS Sustain. Chem. Eng.* **9** 11691–704
[23] Mishra G, Jha R, Rao M D, Meshram A and Singh K K 2021 Recovery of silver from waste printed circuit boards (WPCBs) through hydrometallurgical route: a review *Environ. Chall.* **4** 100073
[24] Reardon-Anderson J 1985 *Science and Civilisation in China: Volume 5. Chemistry and Chemical Technology. Part I. Paper and Printing* vol 108, ed T Tsuen-Hsuin and J Needham (Cambridge: Cambridge University Press) pp 733–5
[25] Wiklund J, Karakoç A, Palko T, Yiğitler H, Ruttik K and Jäntti R 2021 A review on printed electronics: fabrication methods, inks, substrates, applications and environmental impacts *J. Manuf. Mater. Process.* **5** 89
[26] Khan Y, Thielens A, Muin S, Ting J, Baumbauer C and Arias A C 2020 A new frontier of printed electronics: flexible hybrid electronics *Adv. Mater.* **32** 1905279
[27] Garlapati S K, Divya M, Breitung B, Kruk R, Hahn H and Dasgupta S 2018 Printed electronics based on inorganic semiconductors: from processes and materials to devices *Adv. Mater.* **30** 1707600
[28] Li T *et al* 2021 Developing fibrillated cellulose as a sustainable technological material *Nature* **590** 47–56
[29] Zhang Y, Zhang L, Cui K, Ge S, Cheng X and Yan M 2018 Flexible electronics based on micro/nanostructured paper *Adv. Mater.* **30** 1801588
[30] Ahn E, Kim T, Jeon Y and Kim B S 2020 A4 paper chemistry: synthesis of a versatile and chemically modifiable cellulose membrane *ACS Nano* **14** 6173–80
[31] Gaspar C, Sikanen T, Franssila S and Jokinen V 2016 Inkjet printed silver electrodes on macroporous paper for a paper-based isoelectric focusing device *Biomicrofluidics* **10** 064120
[32] Gigac J, Fišerová M, Kováč M and Stankovská M 2020 Paper substrates for inkjet printing of UHF RFID antennas *Wood Res.* **65** 025–36
[33] Gómez N, Quintana E and Villar J C 2014 Effect of paper surface properties on coated paper wettability with different fountain solutions *Biol. Resour.* **9** 4226–41
[34] Ström G 2005 Interaction between offset ink and coated paper—a review of the present understanding *Trans. 13th Fundamental Research Symp.* vol 41 pp 1101–37
[35] Potts S J, Phillips C, Claypole T and Jewell E 2020 The effect of carbon ink rheology on ink separation mechanisms in screen-printing *Coatings* **10** 1008
[36] Gomez E F and Steckl A J 2015 Improved performance of OLEDs on cellulose/epoxy substrate using adenine as a hole injection layer *ACS Photonics* **2** 439–45
[37] Kim J H, Mun S, Ko H U, Yun G Y and Kim J 2014 Disposable chemical sensors and biosensors made on cellulose paper *Nanotechnology* **25** 092001
[38] Kim Y H, Moon D G and Han J I 2004 Organic TFT array on a paper substrate *IEEE Electron Device Lett.* **25** 702–4
[39] Leonat L, White M S, Głowacki E D, Scharber M C, Zillger T, Rühling J, Hübler A and Sariciftci N S 2014 4% efficient polymer solar cells on paper substrates *J. Phys. Chem.* C **118** 16813–7
[40] Kwon S, Oh K, Shin S J and Lee H L 2020 Effects of hydroxyethyl methacrylate comonomer in styrene/acrylate latex on coating structure and printability *Program. Organ. Coat.* **147** 105862
[41] Schuppert A, Thielen M, Reinhold I and Schmidt W A 2011 Ink jet printing of conductive silver tracks from nanoparticle inks on mesoporous substrates *Digital fabrication 2011, NIP27 27th international conference on digital printing technologies: technical program and proceedings* (*Minneapolis, Minnesota, 2–6 October 2011*) pp 437–40
[42] Arbab A A, Arain R A, Qureshi R F, Sahito I A, Sun K C and Jeong S H 2019 Nonwoven polyethylene terephthalate paper loaded with enzyme coupled multiwall carbon nanotubes for superior photocatalytic activity for water remediation *Fiber Polym.* **20** 770–8
[43] Zea M, Moya A, Villa R and Gabriel G 2022 Reliable paper surface treatments for the development of inkjet-printed electrochemical sensors *Adv. Mater. Interfaces* **9** 2200371
[44] Choi K H, Yoo J, Kee Lee C and Lee S Y 2016 All-inkjet-printed, solid-state flexible supercapacitors on paper *Energy Environ. Sci.* **9** 2812–21
[45] Kim J Y, Park S H, Jeong T, Bae M J, Song S, Lee J, Han I T, Jung D and Yu S 2010 Paper as a substrate for inorganic powder electroluminescence devices *IEEE Trans. Electron. Devices* **57** 1470–4
[46] Hakola L, Jansson E, Futsch R, Happonen T, Thenot V, Depres G, Rougier A and Smolander M 2021 Sustainable roll-to-roll manufactured multi-layer smart label *Int. J. Adv. Manuf. Technol.* **117** 2921–34
[47] Asadpoordarvish A, Sandström A, Larsen C, Bollström R, Toivakka M, Österbacka R and Edman L 2015 Light-emitting paper *Adv. Funct. Mater.* **25** 3238–45
[48] Najafabadi E, Zhou Y H, Knauer K A, Fuentes-Hernandez C and Kippelen B 2014 Efficient organic light-emitting diodes fabricated on cellulose nanocrystal substrates *Appl. Phys. Lett.* **105** 063305
[49] Hübler A, Trnovec B, Zillger T, Ali M, Wetzold N, Mingebach M, Wagenpfahl A, Deibel C and Dyakonov V 2011 Printed paper photovoltaic cells *Adv. Energy Mater.* **1** 1018–22
[50] Yang P, Li J, Lee S W and Fan H J 2022 Printed zinc paper batteries *Adv. Sci.* **9** 2103894
[51] Wang C Y, Fuentes-Hernandez C, Chou W F and Kippelen B 2017 Top-gate organic field-effect transistors fabricated on paper with high operational stability *Org. Electron.* **41** 340–4
[52] Gao L, Chao L, Hou M, Liang J, Chen Y, Yu H D and Huang W 2019 Flexible, transparent nanocellulose paper-based perovskite solar cells *npj Flex. Electron.* **3** 1–8
[53] Brooke R, Åhlin J, Hübscher K, Hagel O, Strandberg J, Sawatdee A and Edberg J 2022 Large-scale paper supercapacitors on demand *J. Energy Storage* **50** 104191
[54] Bollström R and Toivakka M 2013 Paper substrate for printed functionality Cambridge 'Anson S J *Trans. of the XVth Fund. Res. Symp.* pp 945–66
[55] Dogome K, Enomae T and Isogai A 2013 Method for controlling surface energies of paper substrates to create paper-based printed electronics *Chem. Eng. Process.: Process Intensif.* **68** 21–25
[56] Kathuria A and Zhang S 2022 Sustainable and repulpable barrier coatings for fiber-based materials for food packaging: a review *Front. Mater.* **9** 929501
[57] Khairuddin Purnawan C and Aningtyas S 2019 Preparation and properties of paper coating based bilayer of starch and shellac composites *J. Phys.: Conf. Ser.* **1153** 012092
[58] Hult E L, Iotti M and Lenes M 2010 Efficient approach to high barrier packaging using microfibrillar cellulose and shellac *Cellulose* **17** 575–86
[59] Shen Z, Rajabi-Abhari A, Oh K, Yang G, Youn H J and Lee H L 2021 Improving the barrier properties of packaging

paper by polyvinyl alcohol based polymer coating—effect of the base paper and nanoclay *Polymers* **13** 1334
[60] Wang L, Wu Z and Cao C 2019 Technologies and fabrication of intelligent packaging for perishable products *Appl. Sci.* **9** 4858
[61] Kopacic S, Walzl A, Zankel A, Leitner E and Bauer W 2018 Alginate and chitosan as a functional barrier for paper-based packaging materials *Coatings* **8** 235
[62] Iotti M, Fabbri P, Messori M, Pilati F and Fava P 2009 Organic–inorganic hybrid coatings for the modification of barrier properties of poly(lactic acid) films for food packaging applications *J. Polym. Environ.* **17** 10–19
[63] García M A, Martino M N and Zaritzky N E 1999 Edible starch films and coatings characterization: scanning electron microscopy, water vapor, and gas permeabilities *Scanning* **21** 348–53
[64] Ma G J, Yoon B K, Sut T N, Yoo K Y, Lee S H, Jeon W Y, Jackman J A, Ariga K and Cho N-J 2022 Lipid coating technology: a potential solution to address the problem of sticky containers and vanishing drugs *View* **3** 20200078
[65] Hoeng F, Bras J, Gicquel E, Krosnicki G and Denneulin A 2017 Inkjet printing of nanocellulose–silver ink onto nanocellulose coated cardboard *RSC Adv.* **7** 15372–81
[66] Bollström R, Määttänen A, Tobjörk D, Ihalainen P, Kaihovirta N, Österbacka R, Peltonen J and Toivakka M 2009 A multilayer coated fiber-based substrate suitable for printed functionality *Org. Electron.* **10** 1020–3
[67] Xu D, Qiu J, Wang Y, Yan J, Liu G S and Yang B R 2017 Chitosan-assisted buffer layer incorporated with hydroxypropyl methylcellulose-coated silver nanowires for paper-based sensors *Appl. Phys. Express* **10** 065002
[68] Atkinson J 2017 Fate of Conductive Ink Pigments during Recycling and Landfill Deposition of Paper-Based Printed Electronics *Ph.D. Thesis* Western Michigan University (available at: https://scholarworks.wmich.edu/dissertations/3144)
[69] Cui J and Zhang L 2008 Metallurgical recovery of metals from electronic waste: a review *J. Hazard. Mater.* **158** 228–56
[70] Gardner Wm H 1936 Plastic properties of shellac *Physics* **7** 306–10
[71] Farag Y and Leopold C S 2009 Physicochemical properties of various shellac types *Dissolution Technol.* **16** 33–39
[72] Sharma S K, Shukla S K and Vaid D N 1983 Shellac-structure, characteristics & modification *Def. Sci. J.* **33** 261–71
[73] Thombare N, Kumar S, Kumari U, Sakare P, Yogi R K, Prasad N and Sharma K K 2022 Shellac as a multifunctional biopolymer: a review on properties, applications and future potential *Int. J. Biol. Macromol.* **215** 203–23
[74] Yuan Y, He N, Xue Q, Guo Q, Dong L, Haruna M H, Zhang X, Li B and Li L 2021 Shellac: a promising natural polymer in the food industry *Trends Food Sci. Technol.* **109** 139–53
[75] Irimia-Vladu M, Głowacki E D, Schwabegger G, Leonat L, Akpinar H Z, Sitter H, Bauer S and Sariciftci N S 2013 Natural resin shellac as a substrate and a dielectric layer for organic field-effect transistors *Greenwich Chem.* **15** 1473
[76] Poulin A, Aeby X, Siqueira G and Nyström G 2021 Versatile carbon-loaded shellac ink for disposable printed electronics *Sci. Rep.* **11** 23784
[77] Htun M, Andersson H and Rigdahl M 1984 The influence of drying strategies on the anisotropy of paper in terms of network mechanics *Fibre Sci. Technol.* **20** 165–75
[78] Sampson W W 2009 Materials properties of paper as influenced by its fibrous architecture *Int. Mater. Rev.* **54** 134–56
[79] Lewis J 2006 Material challenge for flexible organic devices *Mater. Today* **9** 38–45
[80] Grüßer M, Waugh D G, Lawrence J, Langer N and Scholz D 2019 On the droplet size and application of wettability analysis for the development of ink and printing substrates *Langmuir* **35** 12356–65
[81] Kaelble D H 1970 Dispersion-polar surface tension properties of organic solids *J. Adhes.* **2** 66–81
[82] Owens D K and Wendt R C 1969 Estimation of the surface free energy of polymers *J. Appl. Polym. Sci.* **13** 1741–7
[83] Horcas I, Fernández R, Gómez-Rodríguez J M, Colchero J, Gómez-Herrero J and Baro A M 2007 WSXM: a software for scanning probe microscopy and a tool for nanotechnology *Rev. Sci. Instrum.* **78** 013705